XII. MANGANESE NODULES IN THE GH79-1 AREA: GENERAL DESCRIPTIONS

Atsuyuki Mizuno, Kokichi Iizasa, Keiji Handa**, Haruaki Tsuchiya***, and Kenji Ishii****

Introduction

This chapter describes the distribution of morphology, concentration, and occurrence of deep-sea manganese nodules in the GH79-1 area comprising both the main and detailed survey areas, based on our results of field observations. Their most parts were collected from the depths ranging from 5,200 to 5,800 meters, with some exceptions from shallower depth.

In the main survey area, bottom sampling was done at stations spaced over a distance of usually 1° about 110 km apart by a box corer with double spades (Figs. I-4, 8), which can take a bottom portion of about 0.4 m^2 square area and 40 cm deep with little disturbance. At some stations, a box corer with single spade (Fig. I-9) was used. At all the stations, bottom sampling and photographing by two or four sets of freefall grab with camera and small sediment-sampling tube (Figs. I-10, 11) in order to obtain additional data of variabilities of nodule and sediment distributions with in a small area including sampling site by the box corer.

In the detailed survey area, bottom sampling by the box corer, either single spade type or double spade type, was done at stations arranged at an interval of about 19 km, together with additional observations by the freefall grab and camera. Also, sampling and bottom photographing only by freefall grab and camera were done at intervals of 1.9 km and less, to obtain detailed data of local variabilities of nodule distribution along a west-east survey line (Fig. I-6).

Nodule samples obtained were described and studied on board for 1) observation of occurrence and morphology in samplers; 2) measurement of weight and calculation of abundance (in kg/m^2); measurement of size and identification of morphologic type; observation of internal structures of nodule on cut section. Chemical and mineralogical analyses and other works were carried out in the onshore laboratories after the cruise; the results are presented in Chapters XVI, XVIII, XIX, and XX of this cruise report. Coverage of nodules on the sea floor was visually estimated by a percentage chart on board, and the results were revised by the data obtained by a optical image analyser in the onshore laboratory (HANDA and TSURUSAKI, this cruise report). We estimated the abundance of nodules at a station at first on the basis of the calculated data from box core samples. Abundance data based on freefall grab samples were compared with the data of coverage by bottom photographs obtained simultaneously with the grab sampling, and only the data thought to be reliable were used for consideration, because a

*University of Tokyo, Tokyo
**National Research Institute for Pollution and Resources, Tsukuba
***Metal Mining Agency of Japan, Tokyo

freefall grab occasionally does not collect all of the nodule samples within the entire bottom area of the grab.

Results of field observations

The results are summarized in Appendix XII-1, which includes raw data of morphologic type, total weight, abundance, coverage, and size distribution of nodules at each sampling sites, with bathymetric data.

Morphology and occurrence of manganese nodules

Morphological classification of nodules were based on the classification scheme shown in Table XII-1, which were partly modified from MORITANI *et al.*'s scheme (in MIZUNO and MORITANI, *eds.*, 1977).

Manganese nodules from the abyssal basin in the survey area include the morphologic types of Sr, SPr, Dr, Vr, DPr, Ss, SPs, DPs, ISs, IDPs, Ds, DPs(r), etc. We discriminated the types of SPs(r), DPs(r), IDPs(r), and SPr(s). The first to the third types mean the nodules largely covered with smooth surface but with considerable development of rough surface. Inversely, the last one represents the nodules largely having rough surface but with considerable development of smooth surface. Nodules range from about 10 cm to less than 1 cm in diameter. In general, the nodules with rough surface (r-type nodules) tend to be concentrated in the size fractions of 4–2 cm, 2–1 cm, and 1 cm>, with accessory amount of the nodules larger than 6–4 cm, whereas the nodules with smooth surface (s-type nodules) tend to be distributed in wider range including the

Table XII-1 Morphological classification of manganese nodules in the Central Pacific Basin (modified from MORITANI *et al.*, 1977).

Types	Size	Shape	Surface texture
Sr	small to medium	spheroidal/ellipsoidal	rough (granular or microbotryoidal)
SPr	small to medium	spheroidal/ellipsoidal/intergrown	rough
SEr	medium to large	spheroidal/ellipsoidal	rough to botryoidal
Dr	medium to small	discoidal	rough
DPr	small	discoidal/intergrown	rough
Db	medium to large	discoidal/ellipsoidal	rough to botryoidal
DPs	small to medium	flattened/elongated/discoidal/ intergrown	smooth
Ss/SPs	small to medium	spheroidal/intergrown	smooth to microgranular
Ds	small to medium	discoidal	smooth
ISs	large	irregular/spheroidal/flattened/ angular/fractured	smooth
IDPs	large	irregular/flattened/discoidal/ fractured	smooth
V	small to large	variable depending on nucleus forms (shark's teeth, nodule fragments, etc.)	smooth or rough (distinctive form is named Vr or Vs)

Each type name is represented by the symbols taken from the initial of each morphological term, mostly applying the Meylan/Craig's classification method (Meylan, 1974). Here, each size class roughly corresponds in maximum diameter; small-<4 cm, medium-4–6 cm large-> 6 cm. Morphological symbols indicate; S- spheroidal, E-ellipsoidal, D-discoidal, P-poly or intergrown, I-irregular, V-variable, F-faceted, B-biological, T-tabular or flattened.

size fractions larger than 4–2 cm but with less abundance of the nodules of 1 cm>. In result, generally the r-type nodules are smaller than the s-type nodules (Appendix XII-1).

Some of the nodules from the abyssal basin area are illustrated in Fig. XII-1, with their internal structures. Internal structures of the nodules appear to differ according to nodule types. Generally, the r-type nodules lack a nucleus or have small ones, and dendritic colloform structures are developed. The s-type nodules often contain fractures. Nuculeus ranges from very small to very large. Some of the nodules have concentric bands and small nuclei similar to that of the r-type nodules, and other some nodules with larger size consist of internal massive or less clear banded blocks of older nodules and an outer younger thin oxide layer coating (2–3 mm thick). Nuclei of the nodules (both the r- and s-type) are pumice, volcanic rock, phosphatized material, fossil (shark' tooth), and older nodule often fragmented).

Examinations of occurrence of the abyssal nodules on box cores immediately after recovering on the ship and on bottom photographs taken by freefall camera (Fig. XIII-2) give the conclusion that the r-type nodules are burried in larger part but the s-type nodules are shallowly buried in sediments, and thus the former nodules are "burried type" and the latter nodules are "exposed type".

A peculiar type of nodule which was designated as V type was found from the station (St. 1492) on a topographic high at a depth of about 4,200 meters. It is 35 cm × 22 cm × 21 cm in size and very irregularly subrounded, with gritty to granular surface (Fig. XII-2a). Internal structures show that younger ferromanganese layer has grown upon fragmented older large nodule which had been partly phosphatized (Fig. XII-2b). The large nodule was recovered together with five small nodules (less than 4 cm dia.). From the nearby sites (freefall grab sampling and photographing), DPs and V type nodules of 6–1 cm dia. were collected (Appendix XII-1). All the sites including the box core sampling are underlain by calcareous ooze (Table I-6). Field occurrence of the large nodule is unknown, because it was recovered with a great disturbance within the box corer, but it may have rested upon the sea bottom of calcareous ooze, exposing its larger part to the bottom water from the data that the sediment attaches only to a part of the nodule surface.

Distribution of manganese nodules

Nodule distribution in relation to bathymetry is graphically summarized in Fig. XII-3. Various types of nodule in the abyssal basin area occur at the depths ranging from about 4,900 to 5,900 meters. The figure shows that the r-type nodules range from 4,900 to 5,700 meters in depth of occurrence, but the s-type nodules from 5,100 to 5,800 meters. Moreover, abundant occurrence of nodules is limited to 5,200 to 5,600 meters in depth.

Figure. XII-4(a-c) illustrates the distributions of abundance, morphologic types, and coverage of nodules in the main survey area. Figure XII-5 summarizes the distribution of r-type nodules and the area with abundance more than 10 kg/m^2, together with distribution map of Ni plus Cu grade of nodule more than 1 % throughout the entire GH79–1 survey area.

In the main survey area, nodules occur at nearly all the stations with varying abundance

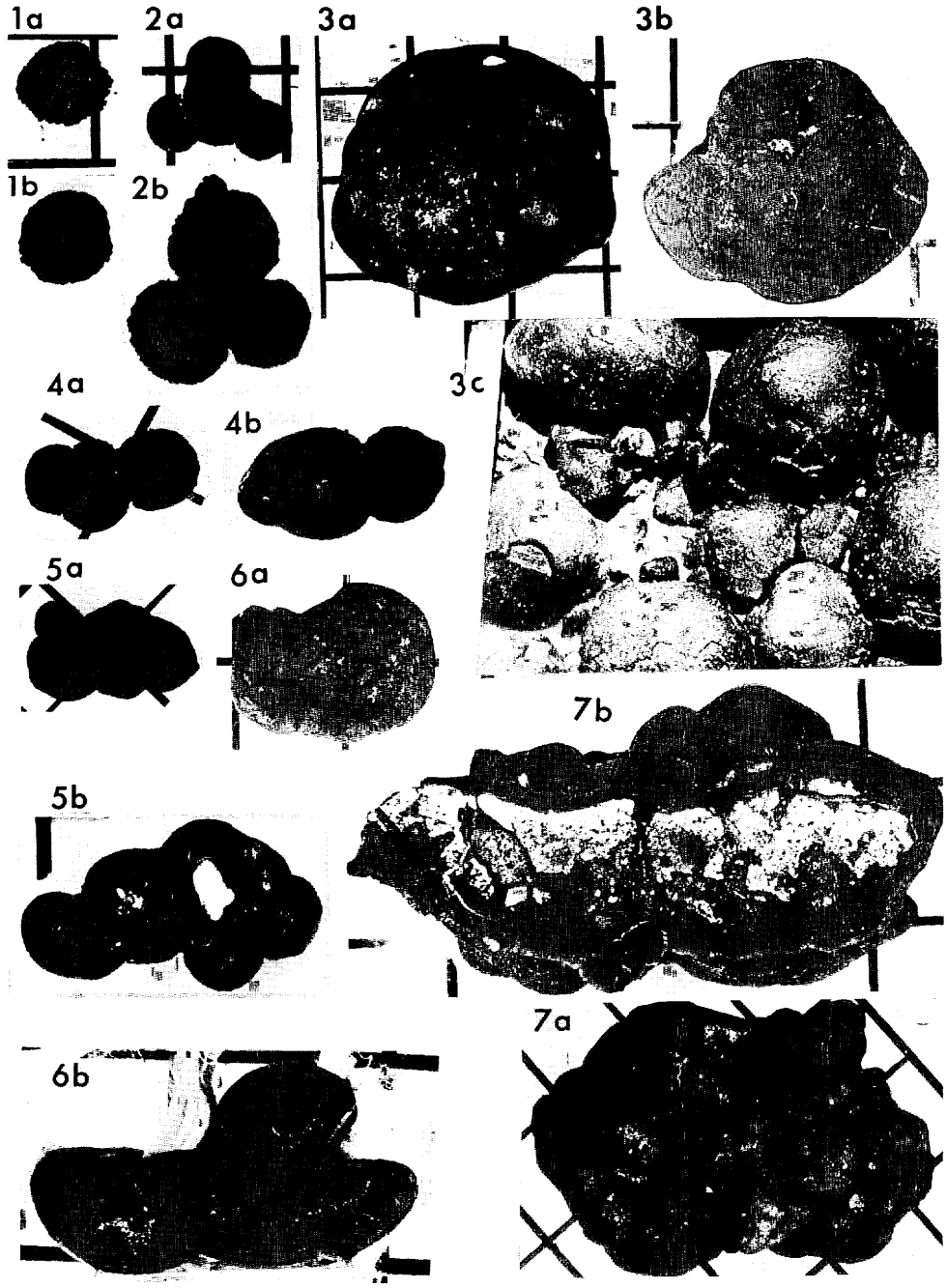

Fig. XII-1 Examples of nodule samples from the GH79-1 area, showing external shape and internal structures.

a: external shape. **b**: internal structures. **c**: occurrence in the box corer. **1** Sr (St. 1476, FG143C-2), **2**, **4** SPr (St. 1484, FG151C-1), **3** Ss (St. 1489, G953), **5** SPs (1481A-1, FG154C-2), **6** DPs (1454, FG121, C-1). Interval of mesh in each figure: 2.5 cm.

a

b

Fig. XII-2 A big nodule from St. 1492. a: external morphology (lateral view). b: internal structures. Lower side of the samples on the photographs show the lower surface of the nodule.

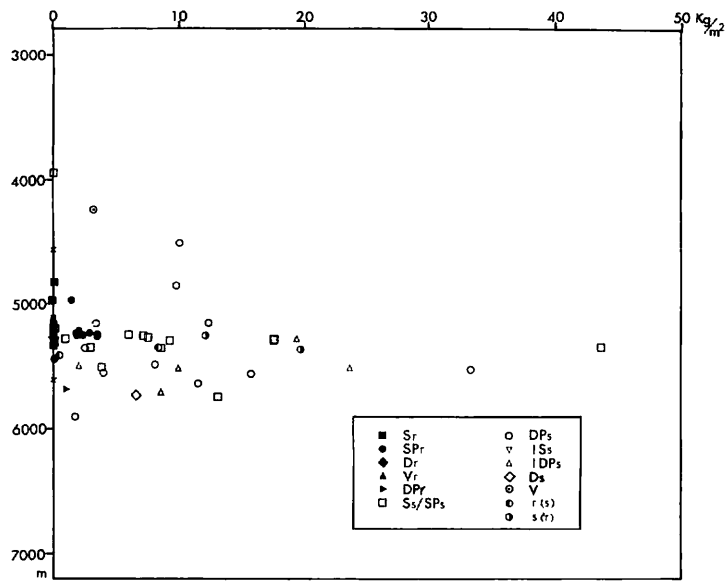

Fig. XII-3 Bathymetric distribution of nodules in the GH79-1 area, with abundance and morphology.

and morphology. Nodules with abundance more than 10 kg/m^2 are distributed in two areas, the central-eastern area and western area, both including the nodule occurrence more than 20 kg/m^2 scatteringly within. The larger part other than the areas yields minor amount of nodules with abundance less than 5 kg/m^2, but the abundance of 5 to 10 kg/m^2 is also found in places within the part. Each morphologic type does not relate to the distribution of abundance above described. However, collectively, the r-type nodules are poorly concentrated with abundance less than 10 kg/m^2, whereas the s-type nodules range very widely and are poorly to very highly concentrated as much as 44 kg/m^2 in abundance. There seems to be no particular correlation between distribution of abundance and morphologic type of nodule and sediment lithology.

Local variability of nodule morphology within each station area is not significant in general. Local variability of abundance or coverage is significantly present in some stations.

In the detailed survey area, manganese nodules of r-type are very poorly concentrated in abundance of less than 1 to 2 kg/m^2 or barren in larger part, and the abundance larger than 10 kg/m^2 is only found at the western part where the s-type nodules are exceptionally distributed in this area (Fig. XII-6). Also, a particular correlation can not be recognized between sediment lithology or bathymetry and abundance-morphology of nodules.

The results of our survey along the 10°N line provide interesting data of local variability of nodule occurrence. Figure XII-7 summarizes the distribution of nodule abundance along the survey line together with a part of the results of chemical analysis of nodules and the interpretation of acoustic records.

The nodule abundance of 19 kg/m^2 at the western end rapidly decreases toward the east, to less than 10 kg/m^2 and 5 kg/m^2 within the distances of approximately 5 km

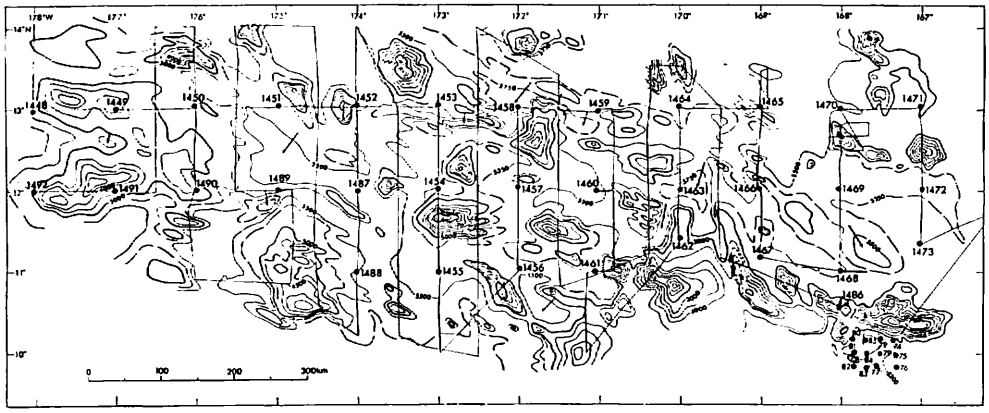

a

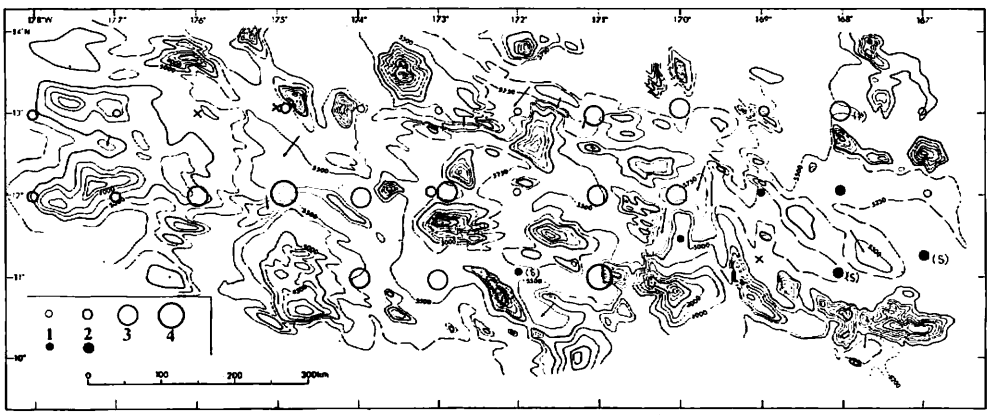

b

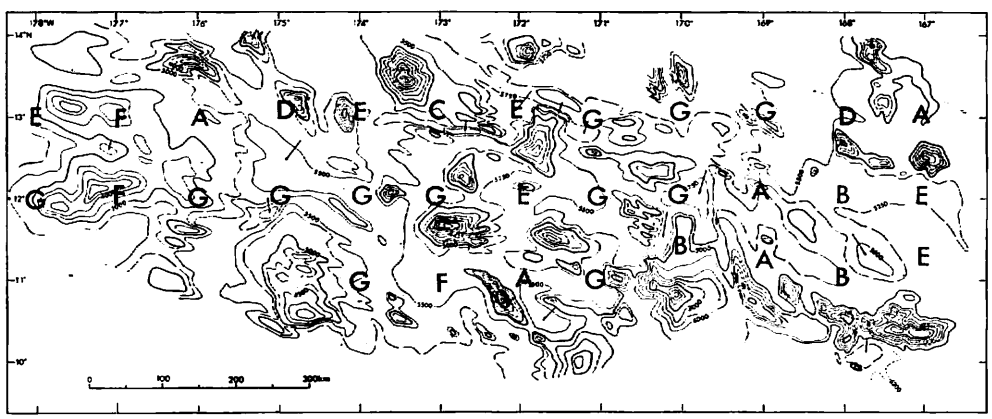

c

Fig. XII-4 Distribution of morphology, abundance, and coverage of manganese nodules in the GH79-1 main survey area.

a: Sampling and bottom-photographing stations. b: Morphology and abundance based on bottom sampling data. Solid and open circles show the r- and s-type nodules, respectively. Abundance is illustrated as follows: 1, 0.1–5 kg/m^2; 2, 5–10 kg/m^2; 3, 10–20 kg/m^2; 4, 20 kg/m^2<. Cross mark shows non occurrence of nodule. c: coverage based on bottom photographs. A, <1; B, 1–10; C, 10–20; D, 20–35; E, 35–50; F, 50–75; G, >75 (in per cent).

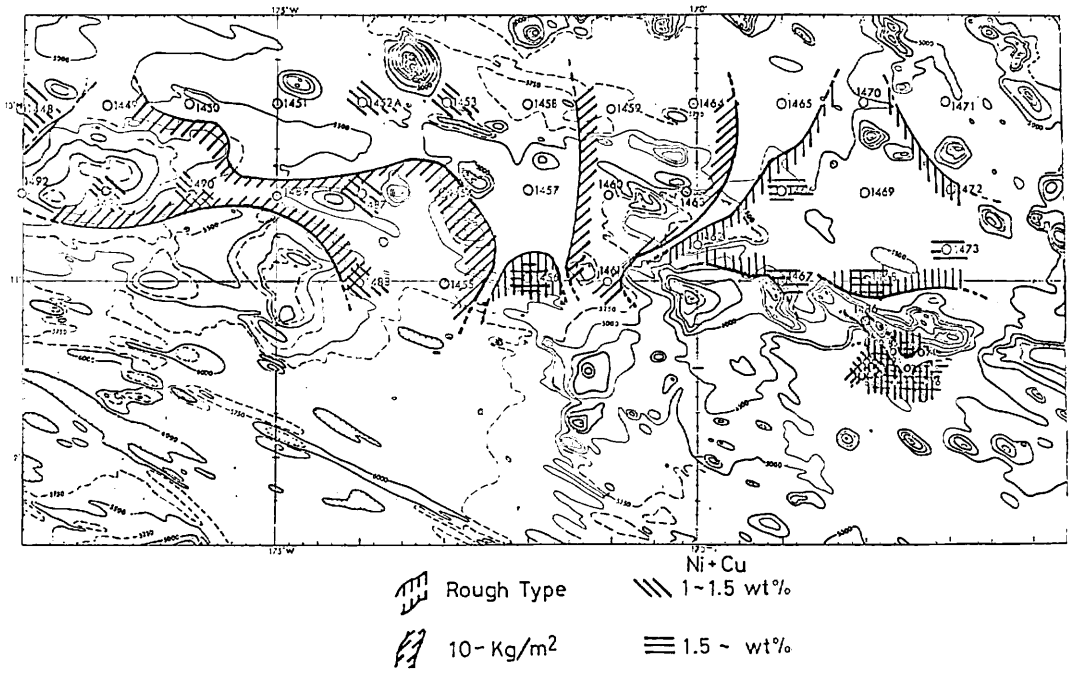

Fig. XII-5 Distribution map of abundance, morphology, and Ni plus Cu grade of nodules in the entire GH79-1 area. Only the area with the nodules of rough group, the area with the abundance more than 10 kg/m^2, and the area of Ni plus Cu grade, 1–1.5% and 1.5< % are demonstrated. Bathymetric map was cited from WINTERER (1972)' one (WINTERER, E., EWING, J.I., *et al.*, 1973).

and 12 km, respectively. The nodules occur only in traceable amount or are barren on the eastern half of the line, east of the site approximately 22 km away from the western end. Nodule morphology varies from place to place, but the following tendency of distribution, showing a definite tendency of serial change of morphology, is found: IDPs type occurs in the highest abundance part (19 kg/m^2) followed by DPs type and SPs type successively with decreasing abundance to 8 kg/m^2; SPs type is followed by SPr type (2 to 7 kg/m^2) and Sr type (less than 1 kg/m^2). The most marked feature is, thus, that the morphologic type varies with the nodule abundance. The s-type nodules are correlated with the abundance higher than about 8 kg/m^2 and the r-type nodules with that less than 7 kg/m^2. As shown in Fig. XII-7, the decreasing of abundance accompanied by the change of morphology is inversely correlated to the increasing of nickel and copper grades and seems to be related to the change of thickness of the latest Pliocene to Quaternary sedimentary sequence. Genetic relation of these correlations will be discussed in Chap. XXIV of this cruise report.

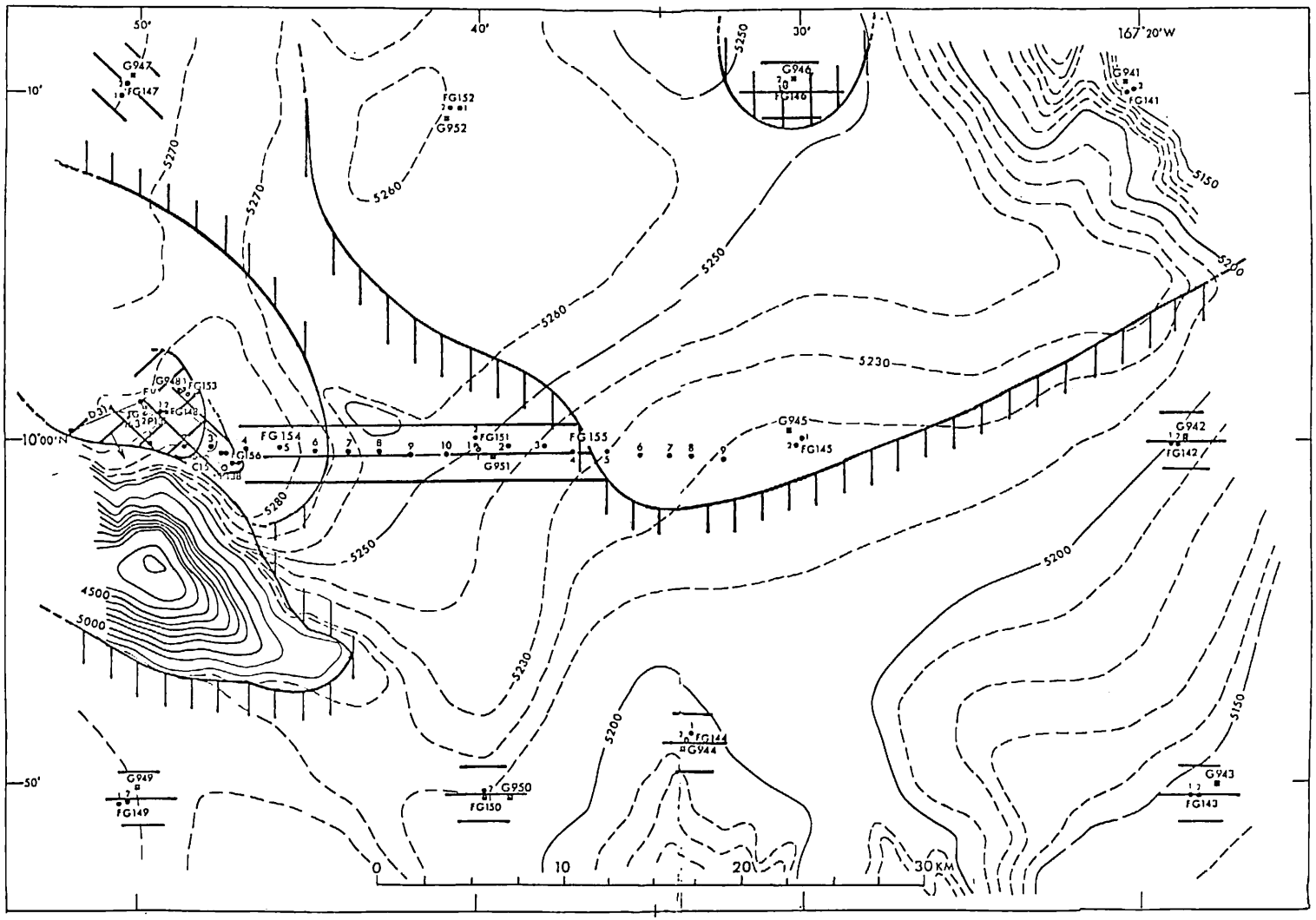

Fig. XII-6 Enlarged distribution map of abundance, morphology, and Ni plus Cu grade of nodules in the detailed survey area around 10°N, 167°40'W. The method of description is same as Fig. XII-5.

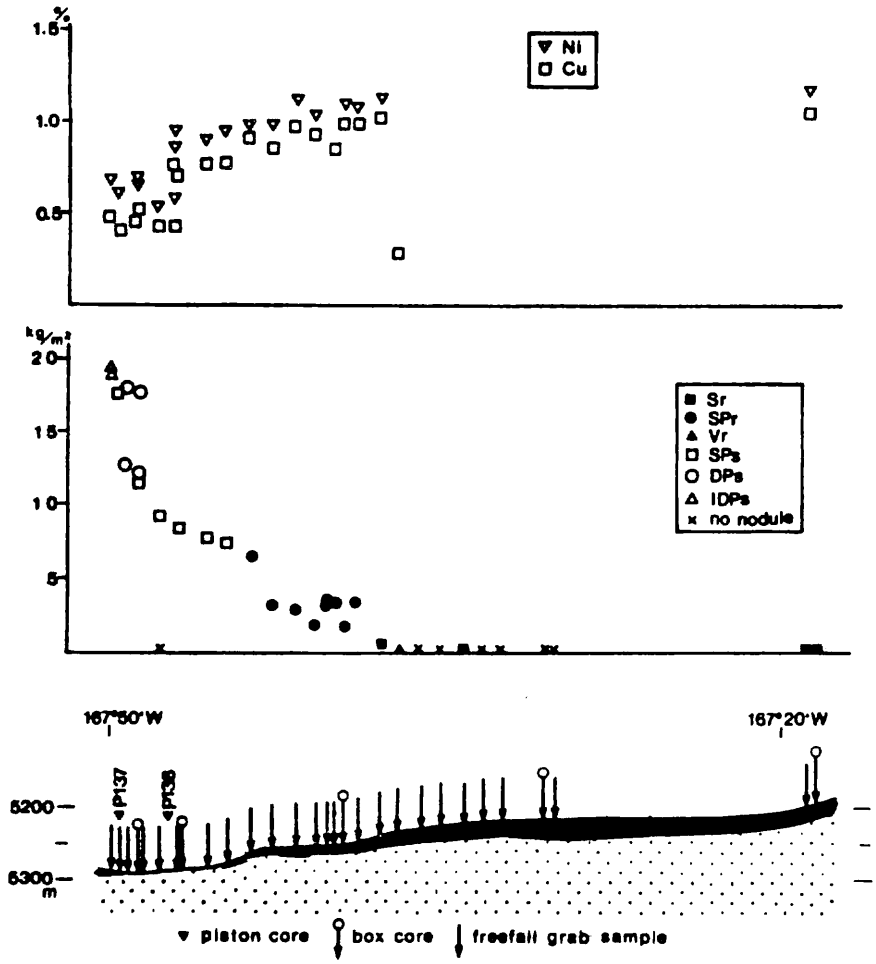

Fig. XII-7 Variability of manganese nodules along the 10°N survey line in the detailed survey area, with an interpretation of acoustic records. From the top to the bottom: distribution of nickel and copper grades; distribution of abundance, with morphologic types; an interpretation of acoustic records.

References

MIZUNO, A. and MORITANI, T. (*eds.*) (1977) Deep sea mineral resources investigation in the central-eastern Central Pacific Basin, August–October 1976 (GH76–1 Cruise). *Geol. Surv. Japan Cruise Rept.*, no. 8, p. 1–217.

WINTERER, E. L., EWING, J. I., *et al.* (1973) *Initial Reports of the Deep Sea Drilling Project*, Vol. 17, Washington (U.S. Government Printing Office), xx + 930p.

Appendix XII-1 List of sampled and observed

Sta. No.	Sample No.	Depth (m)	Dominant morphological type	Total weight (kg)	Abundance (kg/m²)	Coverage* (%)	>10
1448	G(B)915	5171	DPs	0.59 (124)	3.7		
	FG115-1	5165	DPs	0.94 (254)	8.6		
	FG115C-1	5154	SPs	1.03 (187)	9.3	50	
	FG115-2	5154	SPs	0.58 (180)	5.3		
	FG115C-2	5165	DPs	0.59 (98)	5.4	35	
1449	G(B)916A	3957	Ss	2.53 (522)	—		
	FG116-1	3916	SPs	0.07 (13)	0.6		
	FG116C-1	3926	Ss	0.10 (7)	0.9	50	
	FG116-2	3957	Ss	0.26 (31)	2.4		
	FG116C-2	3977	SPs	0.02 (6)	0.1	75	
1450	FG117-1	5118	—	—	—		
	FG117-2	5119	—	—	—		
1451	G(B)918	5502	SPs	— (2)		0	
	FG118-1	5540	IDPs	0.35 (31)	3.2		
	FG118C-1	5541	IDPs	1.09 (77)	9.9	20	0.35(1)
	FG118-2	5505	DPs	0.89 (138)	8.1		
	FG118C-2	5484	DPs	0.90 (122)	8.2	30	
1452	G(B)919	5526	SPs	0.39 (27)	2.4		
	FG119-1	5526	SPs	0.43 (96)	3.9		
	FG119C-1	5532	SPs	0.45 (93)	4.1	40	
	FG119-2	5536	IDPs	0.22 (36)	2.0		
	FG119C-2	5542	SPs	0.23 (51)	2.1	40	
1453	G(B)920	5690	DPr	0.17 (6)	1.0		
	FG120-1	5729	IDPs, V	0.94 (52)	8.6		0.29(1)
	FG120C-1	5729	DPs	0.65 (52)	5.9	20	
	FG120-2	5725	DPs	0.26 (34)	2.4		
	FG120C-2	5722	IDPs, V	0.47 (16)	4.3	20	
1454	G(B)921	5350	DPs	1.31 (151)	8.2		
	FG121-1	5350	DPs	1.70 (218)	15.5		
	FG121C-1	5350	DPs	2.08 (181)	18.9	80	
	FG121-2	5351	DPs	1.75 (202)	15.9		
	FG121C-2	5352	DPs	1.75 (150)	15.9	80	
1455	G(B)922	5557	DPs	0.36 (22)	2.3		
	FG122-1	5554	DPs	1.33 (192)	12.1		
	FG122C-1	5554	SPs/DPs	1.35 (188)	12.5	—	

*Based on the data by a optical image analyser in the onshore laboratory.

manganese nodules, GH79-1 cruise.

Weight of size fraction						Remarks
10–8	8–6	6–4	4–2	2–1	1>	
		0.13(4)	0.35(42)	0.1 (52)	0.01 (26)	
		0.09(2)	0.43(60)	0.39 (173)	0.01 (22)	Broken nodules 0.02 kg
		0.05(2)	0.52(79)	0.25 (103)	0.005(3)	Broken nodules 0.2 kg
	0.08(1)		0.29(59)	0.21 (109)	0.005(11)	Broken nodules 0.04 kg
		0.03(2)	0.4 (54)	0.07 (40)	— (2)	Broken nodules 0.09 kg
			1.58(102)	0.6 (292)	0.05 (128)	Broken nodules 0.3 kg
			0.03(2)	0.035(11)		
		0.05(1)	0.03(2)	0.01 (4)		Broken nodules 0.01 kg
			0.16(12)	0.1 (19)		
			0.01(2)	— (2)	— (2)	
						Broken nodules several grams
						Broken nodules several grams
			— (1)	— (1)		Very small two nodules
	0.03(1)	0.12(7)	0.11(16)	0.02 (5)	— (2)	
0.09(1)	0.22(5)	0.3 (18)	0.14(37)	0.04 (15)		Broken nodules 0.05 kg
		0.23(7)	0.43(83)	0.07 (45)	— (3)	Broken nodules 0.11 kg
						Shark's teeth
		0.15(3)	0.49(62)	0.11 (52)	— (5)	Broken nodules 0.15 kg
						Shark's teeth
		0.03(1)	0.11(12)	0.02 (10)	— (4)	Broken nodules 0.23 kg
		0.06(2)	0.23(37)	0.08 (50)	— (7)	Broken nodules 0.06 kg
		0.01(1)	0.23(42)	0.08 (46)	— (4)	Broken nodules 0.13 kg
		0.04(1)	0.12(13)	0.04 (20)	— (2)	Broken nodules 0.02 kg
			0.11(17)	0.05 (27)	— (7)	Broken nodules 0.07 kg
		0.15(4)	0.02(2)			
0.25(1)		0.10(3)	0.21(29)	0.03 (17)	— (1)	Broken nodules 0.06 kg
		0.09(4)	0.18(33)	0.03 (14)	— (1)	Broken nodules 0.35 kg
		0.04(2)	0.18(24)	0.02 (6)	— (2)	Broken nodules 0.20 kg
0.28(1)		0.10(4)	0.01(3)	0.01 (8)		Broken nodules 0.07 kg
						Shark's teeth five
		0.16(10)	0.98(116)	0.07 (25)		Broken nodules 0.1 kg
		0.13(8)	1.28(168)	0.11 (42)		Broken nodules 0.18 kg
		0.24(12)	1.28(147)	0.08 (22)		Broken nodules 0.48 kg
		0.13(7)	1.13(151)	0.13 (44)		Broken nodules 0.36 kg
						Shark's teeth
		0.18(11)	1.06(138)	0.002(1)		Broken nodules 0.51 kg
		0.07(1)	0.14(6)	0.15 (13)	— (2)	Pumice (880 g)
		0.31(14)	0.88(106)	0.13 (71)	— (1)	Broken nodules 0.01 kg
						Shark's teeth
		0.17(7)	0.98(102)	0.14 (63)	0.02 (16)	Broken nodules 0.04 kg
						Shark's teeth

Appendix XII-1

Sta. No.	Sample No.	Depth (m)	Dominant morphological type	Total weight (kg)	Abundance (kg/m²)	Coverage* (%)	>10
1455	FG122-2	5557	DPs	1.37 (126)	12.5		
	FG122C-2	5556	SPs/DPs	0.35 (31)	3.2	60	
1456	FG123-1	5407	Sr(s)	0.05 (8)	0.5		
	FG123C-1	5407	Sr(s)	0.05 (27)	0.5	1	
	FG123-2	5407	SPr(s)	0.05 (9)	0.5		
	FG123C-2	5407	Sr(s)	0.02 (5)	0.2	1	
1457	G(B)924	5380	DPs	0.40 (155)	2.6		
	FG124-1	5365	DPs	0.84 (161)	7.6		
	FG124C-1	5367	DPs	0.08 (8)	0.7	50	
	FG124-2	5373	DPs	0.55 (103)	5.0		
	FG124C-2	5376	DPs	0.86 (216)	7.8	50	
1458	G(B)925	5900	DPs	0.30 (4)	1.8		
	FG125-1	5904	IDPs	0.68 (55)	6.3		
	FG125C-1	5904	DPs	0.005(1)	+	35	
	FG125-2	5900	DPs	0.007(1)	+		
	FG125C-2	5900	—	0.02 (—)	0.2	?	
1459	G(B)926	5630	DPs	1.84 (255)	11.5		
	FG126-1	5634	DPs	1.44 (145)	13.1		
	FG126C-1	5611	DPs/IDPs	0.63 (83)	(5.7)	85	
	FG126-2	5553	Ss	3.14 (4)	28.6		
1460	G(B)927	5184	DPs	1.96 (115)	12.3	50	0.21(1)
	FG127-1	5186	DPs/IDPs	0.39 (7)	3.5		
	FG127C-1	5184	IDPs	2.65 (125)	24.1	80	
	FG127-2	5181	IDPs	2.75 (121)	25.0		
	FG127C-2	5181	DPs	2.50 (172)	22.7	80	
1461	FG128-1	5523	Ss/SPs	3.53 (42)	32.1		
	FG128C-1	5514	Ss/SPs	3.73 (63)	33.3	85	
	FG128-2	5515	Ss/SPs	2.34 (32)	21.3		
	FG128C-2	5506	Ss/SPs	0.86 (22)	7.8	85	
1462	G(B)929	4846	Sr/SPr	0.07 (48)	0.05		
	FG129-1	4844	Sr	0.01 (7)	0.1		
	FG129C-1	4849	Sr	0.02 (30)	0.2	1	
	FG129-2	4854	DPs	— (1)	+		
	FG129C-2	4854	Sr	0.01 (4)	+	3	
1463	G(B)930	5766	SPs	2.18 (412)	13.6	75	
	FG130-1	5743	SPs	1.09 (70)	9.9		

(Continued)

Weight of size fraction						Remarks
10–8	8–6	6–4	4–2	2–1	1>	
		0.55(35)	0.65(70)	0.05 (19)	— (2)	Broken nodules 0.12 kg
						Shark's teeth
		0.15(6)	0.18(22)	0.05 (3)		Broken nodules 0.03 kg
			0.04(4)	0.01 (4)		
			0.01(3)	0.02 (9)	— (15)	Broken nodules 0.01 kg
		— (1)	— (5)	— (2)	— (1)	Shark's teeth
				— (4)	— (1)	Shark's teeth
		0.02(2)	0.27(46)	0.09 (57)	0.03 (50)	
		0.03(2)	0.55(79)	0.14 (71)	— (9)	Broken nodules 0.12 kg
			0.02(1)	0.04 (5)	— (2)	Broken nodules 0.02 kg
		0.02(2)	0.33(57)	0.10 (42)	— (2)	Broken nodules 0.10 kg
		0.02(1)	0.48(75)	0.23 (125)	0.02 (15)	Broken nodules 0.11 kg
	0.13(2)	0.08(2)				Broken nodules 0.09 kg
0.11(1)	0.07(1)	0.08(3)	0.13(18)	0.05 (32)		Broken nodules 0.24 kg
				— (1)		
				— (1)		
						Small fragments 0.02 kg
		0.25(11)	1.22(141)	0.28 (103)		Broken nodules 0.19 kg
						Shark's teeth
		0.16(8)	0.76(90)	0.14 (47)		Broken nodules 0.38 kg
		0.08(3)	0.46(61)	0.06 (19)		Broken nodules 0.03 kg
	0.23(1)	0.33(3)				Broken nodules 2.58 kg
	0.33(4)	0.51(22)	0.81(80)	0.02 (8)		Broken nodules 0.08 kg
						Shark's teeth
	0.18(2)		0.08(4)	0.01 (1)		Broken nodules 0.12 kg
0.08(1)	0.02(1)	0.93(25)	0.98(81)	0.04 (17)		Broken nodules 0.60 kg
						Shark's teeth
	0.32(3)	0.98(19)	0.86(76)	0.04 (19)		Broken nodules 0.55 kg
	0.13(1)	0.62(19)	1.38(115)	0.08 (27)		Broken nodules 0.29 kg
	0.54(4)	2.23(25)	0.56(13)			Broken nodules 0.52 kg
	0.41(3)	1.78(24)	0.83(34)	0.02 (3)		Broken nodules 0.69 kg
	0.70(4)	1.25(15)	0.26(9)	— (1)		Broken nodules 0.13 kg
		0.68(10)	0.13(7)	0.01 (5)		Broken nodules 0.04 kg
			0.03(1)	0.04 (37)	— (10)	Pumice
				— (7)		
				0.01 (7)	0.01 (23)	
				— (1)		
				— (2)	— (2)	
	0.04(1)	1.12(28)	0.69(63)	0.25 (158)	0.08 (162)	
		0.22(5)	0.73(47)	0.04 (18)		Broken nodules 0.1 kg

Sta. No.	Sample No.	Depth (m)	Dominant morphological type	Total weight (kg)	Abundance (kg/m²)	Coverage* (%)	>10
1463	FG130C-1	5743	SPs	2.10 (106)	19.1	75	
	FG130-2	5743	DPs	0.41 (6)	3.8		
	FG130C-2	5748	SPs	2.41 (73)	21.9	75	
1464	G(B)931	5775	Ds	1.1 (135)	6.9		
	FG131-1	5775	DPs	1.49 (76)	13.6		
	FG131C-1	5775	DPs	1.76 (167)	16.0	85	
	FG131-2	5775	DPs	2.02 (186)	18.4		
	FG131C-2	5775	Ds	1.52 (107)	13.8	85	
1465	G(B)932	5385	SPs	1.34 (256)	8.4		
	FG132-1	5251	—	0.003	+		
	FG132C-1	5238	V, DPs	0.02 (2)	0.2	80	
	FG132-2	5185	DPs/SPs	1.07 (330)	9.8		
	FG132C-2	5172	SPs	0.34 (61)	3.1	80	
1466	G(B)933	5449	SPr/Sr	0.04 (4)	0.2		
	FG133-1	5443	SPr/Sr	0.01 (2)	+		
	FG133C-1	5445	Sr	0.01 (3)	0.1	0	
	FG133-2	5446	Sr	0.01 (3)	+		
	FG133C-2	5442	Sr	— (3)	+	0	
1467	FG134-1	5227	Sr	0.01 (1)	+		
	FG134C-1	5226	—	—	0	0	
	FG134C-2	5225	SPr	0.004(1)	+	0	
1468	FG135-1	5303	Sr	0.05 (5)	0.4		
	FG135C-1	5304	SPs(r)	0.23 (30)	2.1	5	
	FG135-2	5314	Sr	0.01 (3)	0.1		
	FG135C-2	5319	SPs(r)	0.73 (100)	6.6	15	
1469	FG136-1	5359	V	0.02 (7)	0.2		
	FG136C-1	5357	Sr	0.04 (25)	+	5	
	FG136-2	5357	Sr	0.06 (4)	0.6		
	FG136C-2	5362	Sr	— (8)	+	0	
1470	G(B)937	5384	IDPs(r)	3.17 (40)	19.8		2.12(3)
	FG137-1	5505	DPs(r)	0.35 (38)	3.2		
	FG137C-1	5485	DPr/Dr	0.68 (94)	6.2	—	
	FG137-2	5526	Dr	0.06 (7)	0.4		
	FG137C-2	5526	V	0.04 (6)	0.4	25	
1471	G(B)938	5009	—	0.002(—)	(+)		
	FG138-1	5205	SPs	0.48 (85)	4.3		
	FG138C-1	5205	Ds	0.01 (1)	+	0	
	FG138-2	5240	—	0.03 (—)	0.3		
	FG138C-2	5245	Ss, V	0.02 (4)	0.2	0	

(Continued)

Weight of size fraction						Remarks
10–8	8–6	6–4	4–2	2–1	1>	
		0.68(17)	0.78(59)	0.16 (20)		Broken nodules 0.35 kg
		0.07(2)	0.06(3)	— (1)		Broken nodules 0.28 kg
	0.08(1)	0.17(4)	0.68(47)	0.1 (21)		Broken nodules 1.38 kg
						Shark's teeth
		0.22(9)	0.87(107)	0.04 (19)		
		0.26(10)	0.58(24)	0.1 (40)		Broken nodules 0.55 kg
		0.1 (3)	0.78(116)	0.15 (48)		Broken nodules 0.73 kg
		0.13(4)	1.38(130)	0.15 (52)		Broken nodules 0.35 kg
		0.32(8)	0.73(85)	0.04 (14)		Broken nodules 0.43 kg
		0.05(4)	1.16(167)	0.12 (80)	— (5)	
						Small fragments
			0.02(2)			Broken nodules 0.01 kg
			0.88(210)	0.18 (86)	0.10 (34)	
			0.23(31)	0.1 (28)	— (2)	Broken nodules 0.01 kg
		0.02(1)	0.02(2)	— (1)		
			0.01(1)	— (1)		
				0.01 (2)	— (1)	
				0.01 (3)		
				— (3)		
			0.01(1)			
				— (1)		
			0.05(5)			
		0.06(2)	0.14(15)	0.03 (8)	— (5)	
			0.01(1)	— (2)		
0.25(1)		0.12(5)	0.31(32)	0.04 (24)	0.02 (38)	Shark's teeth
				0.02 (4)	— (3)	
		0.02(1)		0.01 (4)	0.01 (20)	Shark's teeth
				0.06 (3)	— (1)	
				— (2)	— (6)	
0.34(1)	0.38(6)	0.15(5)	0.18(17)	— (7)	— (1)	
		0.08(1)	0.13(26)	0.04 (11)		Broken nodules 0.2 kg
		0.14(4)	0.28(48)	0.05 (42)		Broken nodules 0.21 kg
			0.02(1)	0.02 (6)		
			0.04(6)			
						Small fragments
		0.06(2)	0.26(22)	0.12 (52)	0.01 (9)	Broken nodules 0.03 kg
			0.01(1)			
						Small fragments
				0.01 (4)		Broken nodules 0.01 kg

Sta. No.	Sample No.	Depth (m)	Dominant morphological type	Total weight (kg)	Abundance (kg/m²)	Coverage* (%)	>10
1472	G(B)939	5366	V	0.55 (—)	3.4		
	FG139-1	5371	V	0.26 (44)	2.4		0.07(1)
	FG139C-1	5371	—	— (—)	0	30	
	FG139-2	5396	V	0.26 (33)	2.4		0.08(1)
	FG139C-2	5409	V	0.29 (115)	2.6	55	
1473	G(B)940	4992	SPr	0.23 (26)	1.4		
	FG140-1	4983	SPr	1.06 (83)	9.7		
	FG140C-1	4985	SPr(s)	0.82 (65)	7.5	45	0.08(1)
	FG140-2	4983	SPr(s)	0.57 (51)	5.2		
	FG140C-2	4983	S(P)r(s)	0.11 (14)	1.0	50	
1475	G(B)942	5197	DPr	0.01 (2)	+		
	FG142C-1	5198	Sr	0.01 (2)	0.1	0	
1476	G(B')943	5151	Sr	0.05 (20)	0.2	<1	
	FG143C-1	5160	Sr	— (1)	+	0	
	FG143C-2	5160	Sr, SPr	0.1 (7)	0.9	<1	
1477	G(B)944	5197	SPr	0.07 (17)	0.5	1	
	FG144C-1	5208	—	0	0	0	
	FG144C-2	5206	SPr	0.30 (45)	2.7	5	
1478	FG145C-1	5225	—			0	
	FG145C-2	5221	—		0	0	
1479	G(B)946	5259	Dr	0.01 (13)	+		
	FG146C-1	5259	—		0	0	
	FG146C-2	5260	—		0	—	
1480	G(B)947	5256	SPr	0.37 (20)	2.3	3	
	FG147C-1	5253	SPs(r)	0.90 (41)	8.1	15	
	FG147C-2	5252	SPs(r)	0.47 (23)	4.3	15	
1481	G(B')948	5287	DPs(r)	3.05 (183)	12.2	60	
	FG148C-1	5291	(I)DPs	1.98 (114)	18.0	60	
	FG148C-2	5291	SPs	1.38 (173)	12.6	60	
1481A	FG153C-1	5285	IDPs	2.07 (81)	18.9	55	
	FG153C-2	5288	IDPs	2.12 (86)	19.3	55	0.31(1)
	FG153C-3	5289			0	0	
	FG153C-4	5289	SPs	1.27 (150)	11.6	45	
1481A1	FG154C-1	5300	SPs	1.93 (132)	17.6	70	
	FG154C-2	5293	SPs	1.94 (123)	17.7	70	
	FG154C-3	5301	SPs	1.02 (131)	9.2	50	
	FG154C-4	5284	SPs	0.12 (18)	1.1	20	
	FG154C-5	5273	SPs	0.84 (167)	7.6<	15	

(Continued)

Weight of size fraction						Remarks
10–8	8–6	6–4	4–2	2–1	1>	
						Broken nodules
0.03(1)		0.07(3)	0.05(9)	0.03 (18)	— (8)	Broken nodules 0.003 kg
						Zeolitic concretion
0.04(2)		0.04(12)	0.04(10)	0.01 (4)	— (4)	
	0.01(1)	0.03(3)	0.14(31)	0.1 (54)	0.01 (26)	Broken nodules 0.003 kg
		0.09(5)	0.13(15)	0.01 (5)	— (1)	
		0.48(16)	0.53(44)	0.05 (16)	— (7)	
0.03(1)	0.05(2)	0.18(10)	0.37(32)	0.03 (10)	— (9)	Broken nodules 0.09 kg
		0.16(4)	0.34(30)	0.03 (16)	— (1)	Broken nodules 0.04 kg
			0.08(10)	0.01 (3)	— (1)	Broken nodules 0.02 kg
			0.01(1)		— (1)	
				0.01 (2)		
			0.04(12)	— (1)	0.01 (7)	Shark's teeth and pumice
				— (1)		
			0.1 (6)	— (1)		
			0.06(6)	0.01 (4)	0.01 (7)	
						Pumice 2
			0.21(18)	0.08 (19)	0.01 (8)	
				0.01 (7)	— (6)	Pumice
		0.14(5)	0.22(14)	— (1)		
		0.42(15)	0.31(23)	0.01 (3)		Broken nodules 0.16 kg
		0.18(6)	0.23(15)	0.01 (2)		Broken nodules 0.05 kg
	0.26(4)	1.66(59)	1.08(101)	0.05 (17)	— (2)	Pumice
	0.20(2)	0.64(22)	1.00(77)	0.04 (13)		Broken nodules 0.1 kg
		0.13(7)	1.10(125)	0.11 (35)	0.01 (6)	Broken nodules 0.04 kg
0.34(2)	0.26(3)	0.32(9)	0.62(59)	0.02 (8)		Broken nodules 0.51 kg
0.48(2)	0.23(2)	0.28(8)	0.06 (61)	0.03 (12)		Broken nodules 0.13 kg
						Pumice
	0.14(2)	0.23(12)	0.80(87)	0.10 (40)	— (9)	
0.13(1)	0.25(3)	0.65(25)	0.81(81)	0.05 (22)		Broken nodules 0.04 kg
		0.72(28)	0.98(84)	0.04 (11)		Broken nodules 0.20 kg
0.06(1)	0.10(4)	0.25(10)	0.51(64)	0.09 (42)	0.01 (10)	
		0.01(1)	0.10(13)	0.01 (4)		
		0.03(2)	0.65(87)	0.13 (51)	0.02 (27)	Broken nodules 0.01 kg
						Shark's teeth

Sta. No.	Sample No.	Depth (m)	Dominant morphological type	Total weight (kg)	Abundance (kg/m²)	Coverage* (%)	>10
1481A1	FG154C-6	5253	SPs	0.80 (148)	7.3	25	
	FG154C-7	5247	SPr	0.73 (135)	6.6	15	
	FG154C-8	5249	SPr(s)	0.35 (66)	3.2	5	
	FG154C-9	5254	SPr	0.32 (94)	2.9	10	
	FG154C-10	5251	SPr	0.20 (45)	1.9	0	
1481A2	FG156C-1	5293	SPs	0.07 (12)	0.6	40	
	FG156C-2	5288	SPs	— (1)	+	40	
	FG156C-4	5269	SPs	0.66 (164)	6.0	30	
1482	G(B)949	5222	SPr	0.32 (47)	2.0		
	FG149C-2	5220	Sr	0.07 (17)	0.6	0	
1483	G(B)950	5211	SPr	0.34 (55)	2.1	5	
	FG150C-1	5210	SPr(Sr)	0.60 (92)	5.5	5	
	FG150C-2	5211	Sr(DPr)	0.12 (12)	1.1	—	
1484	G(B′)951	5244	SPr	0.46 (103)	1.8	5	
	FG151C-1	5250	SPr	0.40 (83)	3.6	3	
	FG151C-2	5252	SPr	0.37 (84)	3.3	3	
1484A1	FG155C-1	5251	SPr	0.40 (101)	3.6	10	
	FG155C-2	5248	SPr	0.39 (91)	3.5	10	
	FG155C-3	5242	Sr	0.06 (25)	0.5	0	
	FG155C-4	5237	Vr	— (1)	+	0	
	FG155C-5	5231	—		0	0	
	FG155C-6	5228	—		0	0	
	FG155C-7	5223	Sr	— (2)	+	0	
	FG155C-8	5223	—		0	0	
	FG155C-9	5220	—		0	0	
1485	FG152C-1	5259	—		0	0	
	FG152C-2	5262	—		0	0	
1486	D315	1609	IDPs	0.90 (1)	—		0.60(1)
1452A	FG158C-1	5588	—	0.02 (—)	0.2	70	
	FG158C-2	5567	V, DPs	0.44 (200)	4.0	90**	
1487	FG159C-1	5608	D(P)s	1.75 (132)	15.9	75	
	FG159C-2	5614	DPs	2.09 (201)	19.0	90	
1488	FG160C-1	5534	ID(P)s	1.94 (74)	17.6	80	

**including pebbles of rock.

(Continued)

Weight of size fraction						Remarks
10–8	8–6	6–4	4–2	2–1	1>	
		0.03(2)	0.60(87)	0.13 (49)	0.01 (10)	Broken nodules 0.03 kg
		0.10(6)	0.54(76)	0.07 (30)	0.02 (23)	
		0.04(3)	0.26(34)	0.05 (20)	0.01 (9)	Broken nodules 0.35 kg
						Star fish
		0.06(3)	0.2 (29)	0.04 (18)	0.02 (44)	
		0.02(1)	0.12(17)	0.06 (24)	— (3)	
			0.05(6)	0.02 (6)		
				— (1)		
		0.01(1)	0.46(70)	0.18 (80)	0.01 (13)	Pumice
			0.27(23)	0.05 (17)	— (7)	
			0.04(4)	0.03 (8)	— (5)	
		0.02(1)	0.29(33)	0.03 (11)	0.01 (7)	Pumice
		0.19(1)	0.30(30)	0.09 (29)	0.02 (32)	Shark's teeth
		0.09(2)	0.02(2)	0.01 (4)	— (4)	Broken nodules 0.01 kg
		0.01(1)	0.33(48)	0.11 (50)	— (4)	Pumice
			0.31(38)	0.08 (30)	0.01 (15)	
			0.30(40)	0.05 (22)	0.02 (22)	Pumice
		0.02(1)	0.30(40)	0.07 (36)	0.01 (24)	Shark's teeth, pumice
		0.04(1)	0.21(26)	0.13 (47)	0.01 (17)	
			0.02(4)	0.03 (15)	0.01 (6)	
				— (1)		Pumice
						Pumice
				— (1)	— (1)	Pumice
						Crust type; broken nodules 0.30 kg, Blackcord and brittle star
						Broken nodules
	0.06(1)	0.17(4)	0.07(11)	0.07 (51)	0.04 (133)	Broken nodules 0.03 kg
						Pebbles of older rocks
		0.48(26)	0.84(96)	0.03 (10)		Broken nodules 0.4 kg
		0.66(34)	0.98(116)	0.13 (51)		Broken nodules 0.32 kg
						Shark's teeth
	0.25(3)	0.95(33)	0.50(38)			Broken nodules 0.24 kg

Appendix XII-1

Sta. No.	Sample No.	Depth (m)	Dominant morphological type	Total weight (kg)	Abundance (kg/m²)	Coverage* (%)	>10
1488	FG160C-2	5538	(I)D(P)s	2.61 (142)	23.7	80	
1489	G(B)953	5370	Ss	7.01 (233)	43.8	80	
	FG161C-1	5383	—	—	—	80	
	FG161C-2	5362	—	—	—	—	
1490	G(B)954	4877	DPs	1.59 (237)	9.9	75	
	FG162C-1	4853	(I)DPs/Vs	1.72 (27)	15.7	75	
	FG162C-2	4863	(I)DPs	0.98 (75)	8.9	75	
1491	G(B)955	4517	DPs	1.61 (235)	10.0	75	
	FG163C-1	4566	—	—	—	35	
	FG163C-2	4529	DPs	0.13 (9)	1.2	75	
1492	G(B)956	4239	V	10.53 (6)	—		10.5 (1)
	FG164C-1	4225	DPs	0.79 (41)	7.2	80	
	FG164C-2	4227	V	0.24 (40)	2.2	90	

(Continued)

Weight of size fraction						Remarks
10–8	8–6	6–4	4–2	2–1	1>	
	0.41(6)	0.90(36)	0.90(95)	0.01 (5)		Broken nodules 0.39 kg
	4.03(20)	1.96(24)	0.89(96)	0.09 (38)	0.02 (55)	
						No nodule in sampler
						No nodule in sampler
		0.41(23)	1.08(173)	0.06 (29)	0.01 (12)	Broken nodules 0.04 kg
	0.08(1)	0.44(16)	0.65(82)	0.02 (10)		Broken nodules 0.53 kg
		0.20(8)	0.45(56)	0.03 (11)		Broken nodules 0.30 kg
		0.38(16)	1.08(153)	0.11 (54)	0.01 (12)	Broken nodules 0.02 kg
						No nodule zeolite 0.013 kg
		0.01(1)	0.05(7)	— (1)		Broken nodules 0.08 kg
			0.03(4)	— (1)		Nodule (>10) = 35 × 22 × 21 cm
		0.33(10)	0.45(28)	0.01 (3)		
		0.01(1)	0.19(21)	0.03 (13)	— (5)	